

Spatial and Kinematical Lopsidedness of Atomic Hydrogen in the Ursa Major Group of Galaxies

R.A.Angiras¹*, C.J.Jog²,K.S.Dwarakanath³,M.A.W. Verheijen⁴

¹School of Pure and Applied Physics,M.G. University, Kottayam, 686560,India

²Department of Physics, Indian Institute of Science, Bangalore, 560012, India

³Raman Research Institute, Bangalore, 560080, India

⁴Kapteyn Astronomical Institute, Rijksuniversiteit Groningen,Netherlands

(E-mails:rangiras@rri.res.in,cj jog@physics.iisc.ernet.in,dwaraka@rri.res.in,verheyen@astro.rug.nl)

Accepted.....; Received

ABSTRACT

We have carried out the harmonic analysis of the atomic hydrogen (HI) surface density maps and the velocity fields for 11 galaxies belonging to the Ursa Major group, over a radial range of 4-6 disc scalelengths in each galaxy. This analysis gives the radial variation of spatial lopsidedness, quantified by the Fourier amplitude A_1 of the $m=1$ component normalised to the average value. The kinematical analysis gives a value for the elongation of the potential to be $\sim 10\%$. The mean amplitude of spatial lopsidedness is found to be ~ 0.14 in the inner disc, similar to the field galaxies, and is smaller by a factor of ~ 2 compared to the Eridanus group galaxies. It is also shown that the the average value of A_1 does not increase with the Hubble type, contrary to what is seen in field galaxies. We argue that the physical origin of lopsidedness in the Ursa Major group of galaxies is tidal interactions, albeit weaker and less frequent than in Eridanus. Thus systematic studies of lopsidedness in groups of galaxies can provide dynamical clues regarding the interactions and evolution of galaxies in a group environment.

Key words: galaxies: kinematics and dynamics - galaxies: evolution - galaxies: ISM - galaxies: spiral - galaxies: structure - galaxies: groups-galaxies:general

1 INTRODUCTION

It is well-known that the distribution of the atomic hydrogen gas (HI) in many spiral galaxies is non-axisymmetric or lopsided. This lopsidedness was first studied by Baldwin, Lynden-Bell, & Sancisi (1980). From the analysis of global profiles of HI using single dish radio telescopes, it was concluded that over 50 % of galaxies studied show such asymmetry (Richter & Sancisi 1994, Haynes et al. 1998, Matthews, van Driel, & Gallagher 1998). Due to the lack of spatial resolution, such studies could only reveal the combined effect of spatial and velocity asymmetry. The lopsidedness has also been observed kinematically, as in terms of asymmetric rotation curves (Swaters et al. 1999) which can be directly used to obtain the lopsided perturbation potential (Jog 2002). The kinematical asymmetry has been used to deduce the ellipticity of the potential from the analysis of the HI velocity fields (Franx, van Gorkom, & de Zeeuw 1994; Schoenmakers et al. 1997).

Many theories have been proposed for the observed lopsidedness. They include tidal interactions (Jog 1997), minor mergers (Zaritsky & Rix,1997), asymmetric gas accretion (Bournaud et al. 2005), and offset stellar disc in the halo potential (Noordermeer et al. 2001). It is not yet clear which of these possible scenarios work at scales of a galactic group.

Recently, in a first such study, the 2-D spatial distribution of HI was Fourier-analysed to measure the lopsidedness for a sample of 18 galaxies in the Eridanus group of galaxies (Angiras et al. 2006, here onwards called Paper I). In this paper, it was found that the mean amplitude of measured lopsidedness is large ~ 0.2 (i.e., a surface density contrast of 20% above an uniform disc), nearly twice of that seen in the stellar component of the field galaxies (Rix & Zaritsky 1995, Bournaud et al. 2005). Also, it was shown that the early-type spiral galaxies show a higher lopsidedness than the late-type spirals, which is contrary to that observed in field galaxies (Bournaud et al. 2005). These two results suggest that tidal interactions play a dominant role in the generation of lopsidedness in the galaxies in groups, as was argued in paper I. It

* On leave from St. Joseph's College, Bangalore, India

is not known whether these results are common to all group environments, especially since the groups are known to exhibit a large variety of properties (Rasmussen et al. 2006), especially regarding the galaxy density and velocity dispersions.

Here we address this issue by analysing the 2-D HI data for galaxies in the Ursa Major group. The velocity dispersion, the fraction of early type galaxies and the lack of HI deficiency (Verheijen & Sancisi 2001; Omar & Dwarakanath, 2005a) are the major differences between the Ursa Major and the Eridanus groups. Thus the galaxies in the Ursa Major group provide an opportunity to study lopsidedness in a different physical environment. We have selected 11 spiral galaxies belonging to the Ursa Major Group for estimating the spatial lopsidedness and elongation. The spatial lopsidedness values are compared with the results of the Eridanus group of galaxies (Paper I) to see whether group environments give rise to similar values for the amplitudes and phases of the spatial asymmetries. The higher order Fourier components ($m=1,2,3$) have also been obtained. Further, we have carried out an analysis of the kinematical data to estimate the elongation in the potential. This is compared with the values obtained from the spatial analysis. As in the Eridanus case (Paper I), the use of HI as a tracer allows us to study lopsidedness to outer disks covering a radial distance larger than twice that studied earlier using the near-IR data on stars as in Rix & Zaritsky (1995) and Bournaud et al. (2005).

This paper is organised as follows. In section 2 we discuss the HI and optical data used for the proposed analysis. Details of the harmonic analysis, and the results are presented in section 3. A discussion of these results in the context of the group environment is given in section 4 and in section 5 we give the conclusions.

2 DATA

2.1 The Ursa Major Group

The Ursa Major group in the super galactic co-ordinate system lies between $58.53 \leq SGL \leq 73.53$ degrees and $-4.46 \leq SGB \leq 10.54$ degrees (Tully et al. 1996). The systemic velocity of this group is 950 km s^{-1} with a dispersion of 150 km s^{-1} (Verheijen & Sancisi 2001). Seventy nine galaxies have been associated with this group (Tully et al. 1996) and this group had a projected density of $3 \text{ galaxies per Mpc}^{-2}$. Due to the small velocity dispersion, it is not yet clear whether it can be classified as a cluster as mentioned in Tully et al.(1996). In addition this group contains a smaller fraction of early-type galaxies ($\sim 14\%$ (E+S0) and a larger fraction of late-type galaxies $\sim 86\%$ (Sp+Irr)(Tully et al. 1996)) This system does not show a central concentration (Verheijen & Sancisi 2001) which is atypical for a cluster and more similar to that found in a group.

As we shall be using the results from a similar analysis carried out on Eridanus group by Angiras et al. (2006) in section 3&4, a brief summary of the characteristics of this group is given. This group in super-galactic co-ordinate system lies between $\sim -30 \leq SGL \leq -52$ degrees and $272 \geq SGB \geq 292$ degrees at a mean distance of $\sim 23 \pm 2 \text{ Mpc}$. Approximately 200 galaxies are

associated with this group with a velocity dispersion of $\sim 240 \text{ km s}^{-1}$. In this case the projected density was higher, $\sim 8 \text{ galaxies per Mpc}^{-2}$ (Omar & Dwarakanath, 2005a). Unlike Ursa Major, in Eridanus group there was a larger fraction of elliptical and S0 type galaxies ($\sim 30\%$ (E+S0) and a smaller fraction of the late-type galaxies $\sim 70\%$ (Sp+Irr) (Omar & Dwarakanath, 2005a)). In this case also, like Ursa Major, the group centre is not known. The selection criteria for the 18 galaxies that were used for the harmonic analysis by Angiras et al. (2006) are similar to what is given in section 2.2 (paragraph 1).

Even though, these two groups are almost at the same distance from us they differ mainly in two aspects. Firstly, in Eridanus group, HI deficiency is seen which is ascribed to tidal interactions (Omar & Dwarakanath, 2005b). HI deficiency is not seen in the case of Ursa Major (Verheijen & Sancisi 2001). Secondly, compared to Eridanus, Ursa Major is a loose group (Tully et al. 1996; Omar & Dwarakanath, 2005a).

The higher number density and the higher velocity dispersion as seen in the Eridanus group implies a higher rate of tidal interactions between the galaxies in the group. Also, the higher fraction of early-type galaxies seen in the Eridanus represent an earlier evolution of galaxies via tidal interactions. These agree with the higher amplitude of lopsidedness seen in the Eridanus galaxies, if generated by tidal interactions. We caution, however, that the spatial distribution of the Ursa Major galaxies is that of an elongated filament (Tully et al. 1996). Hence, it may not be so straightforward to calculate the dependence of the galaxy interaction rate on the number density in that case.

2.2 Radio Data

Out of the 49 galaxies observed using the Westerbork Synthesis Radio Telescope (WSRT) by Verheijen and Sancisi (2001) , we have selected 11 galaxies on the basis of their inclination and quality of HI maps (galaxies, whose HI maps were patchy were rejected) for further analysis. The right ascension (α), declination (δ), systemic velocity (V_{sys}), inclination (i) and Position Angle (PA) of these galaxies are given in Table 1. All the galaxies selected were in the inclination range of 45 to 70 degrees. This was to ensure the availability of good resolution in velocity maps and HI maps, both of which were essential for the analysis (Block et al. 2002; Bournaud et al. 2005). Details of the observation and the preliminary data reduction are given elsewhere (Verheijen & Sancisi 2001).

For the sake of completeness, a brief summary of the data reduction procedure is given here. As a result of observation of typical duration of 12 to 60 hour with WSRT, raw UV data were obtained. These data were calibrated, interactively flagged and Fast Fourier Transformed using the NEWSTAR software. The resulting data cubes were further processed using the Groningen Image Processing SYstem (GIPSY). All the data cubes were smoothed to $30'' \times 30''$ and continuum subtraction was carried out. The resulting cubes were used to derive the HI-surface density (Moment 0) and HI-velocity (Moment 1) maps. The typical 3σ column density of 10^{20} cm^{-2} was obtained for the moment 0 maps. The moment 1 maps had typical velocity resolution of $\sim 19 \text{ km s}^{-1}$. It should be emphasised that the Eridanus angu-

Table 1. The sample of galaxies selected for spatial lopsidedness analysis (Verheijen & Sancisi 2001)

Name	Hubble Type	$\alpha(\text{J2000})$ h m s	$\delta(\text{J2000})$ ° ' "	V_{sys} (km s $^{-1}$)	Inclination (°)	Position Angle (°)
UGC 6446	Sd	11 26 40.4	53 44 48	644.3	54	200
NGC 3726	SBc	11 33 21.2	47 01 45	865.6	54	194
NGC 3893	Sc	11 48 38.2	48 42 39	967.2	49	352
NGC 3949	Sbc	11 53 41.4	47 51 32	800.2	54	297
NGC 3953	SBbc	11 53 48.9	52 19 36	1052.3	62	13
UGC 6917	SBd	11 56 28.8	50 25 42	910.7	59	123
NGC 3992	SBbc	11 57 36.0	53 22 28	1048.2	58	248
UGC 6983	SBcd	11 59 09.3	52 42 27	1081.9	50	270
NGC 4051	SBbc	12 03 09.6	44 31 53	700.3	50	311
NGC 4088	Sbc	12 05 34.2	50 32 21	756.7	71	231
NGC 4389	SBbc	12 25 35.1	45 41 05	718.4	50	276

lar resolution of $20''$ (~ 2.24 kpc) and velocity resolution (~ 10 kms) and column density (Omar & Dwarakanath, 2005a) were comparable to that of Ursa Major.

2.3 Optical and Near-IR Data

The K'-Band and R-Band images of a few of the largest galaxies having a typical diameter of $3' - 6'$ in the inclination range of $49^\circ - 62^\circ$ were sourced from the Canadian Astronomy Data Centre (CADC) archives. These images were obtained using various telescopes and CCD cameras by Tully et al. (1996) and is kept in the archives after the initial data reductions like cosmic ray removal, dark subtraction, and flat fielding were carried out. The typical resolution of the images were $1''$ (R-Band) and $\sim 2''$ (K-Band). These are analysed to obtain the asymmetry in the stellar distribution, and compare that with the HI asymmetry (Section 3.2).

3 HARMONIC ANALYSIS

3.1 Harmonic Analysis of Radio Data

We have adopted the harmonic analysis for analysing the data (Paper I). In HI, where both velocity maps and surface density maps are available, the analysis technique is different from that adopted in optical analysis. The procedure assumes that in an ideal galaxy, HI is in pure circular motion. Hence we have,

$$V(x, y) = V_0 + V_c \cos(\phi') \sin(i) + V_r \sin(\phi') \sin(i) \quad (1)$$

where $V(x, y)$ is the velocity at the rectangular coordinate (x, y) , V_0 is the systemic velocity, V_c is the rotation velocity, i is the inclination and V_r is the expansion velocity which was taken to be zero. The azimuthal angle (ϕ') measured in the plane of the galaxy, is given by the equations

$$\cos(\phi') = \frac{-(x - x_0) \sin(PA) + (y - y_0) \cos(PA)}{r} \quad (2)$$

$$\sin(\phi') = \frac{-(x - x_0) \cos(PA) + (y - y_0) \sin(PA)}{r \cos(i)} \quad (3)$$

where $r = \sqrt{((x - x_0)^2 + (y - y_0)^2 / \cos(i)^2)}$. In these equations, (x_0, y_0) is the kinematical centre of the galaxy, PA is the position angle of the galaxy measured in the

anti-clockwise direction from the north direction. Using these equations, the five unknown parameters, namely (x_0, y_0) , PA , V_c and i were estimated using the GIPSY task ROTCUR (Baldwin et al. 1980) in an iterative manner (Wong et al. 2003; Omar & Dwarakanath, 2005a). It was observed that the dynamical centre, derived from velocity maps were less than $2''$ away from the optical centre. Hence, for all the calculations the optical centre was used.

3.1.1 Spatial Lopsidedness and Other Non-axisymmetry in HI

The harmonic coefficients were derived from the surface density maps, assuming that the surface density at each radii can be expanded in the form

$$I(r, \phi') = a_0(r) + \sum_m a_m \cos m[\phi' - \phi_m(r)] \quad (4)$$

Here, a_m is the amplitude of the surface density harmonic coefficient and $\phi_m(r)$ is the phase. The harmonic coefficients so derived were normalised using the mean surface density (a_0) at each radius. The variation of the normalised amplitude of the first order harmonic coefficient $A_1 (= a_1/a_0)$ and of the phase angle ϕ_1 with respect to the radius are shown (Figures 1 & 2). The values for the average A_1 measured in the larger range $1.5 - 2.5 R_{K'}$ is given in column 4 of table 2. These values can be compared with the values estimated by earlier workers (Paper I 2006; Bournaud et al. 2005; Rix & Zaritsky 1995). Similarly the values of the fractional Fourier amplitudes A_1 , A_2 , and A_3 corresponding respectively to the Fourier components $m=1,2,3$ in the range $1-2 R_w$ are given in Table 2 (columns 6,7 & - see Section 3.3).

The results from Figs. 1-2 and Table 2 can be summarised as:

- (i) The amplitude of disk lopsidedness shows an increase with radius, and the phase is nearly constant with radius as also seen earlier for the field galaxies (Rix & Zaritsky 1995), and the group galaxies (Paper I). We note, however, that these correlations are not so robust in the Ursa Major case. These similarities, and the differences, provide important clues to the origin of the lopsidedness in the field and group galaxies.

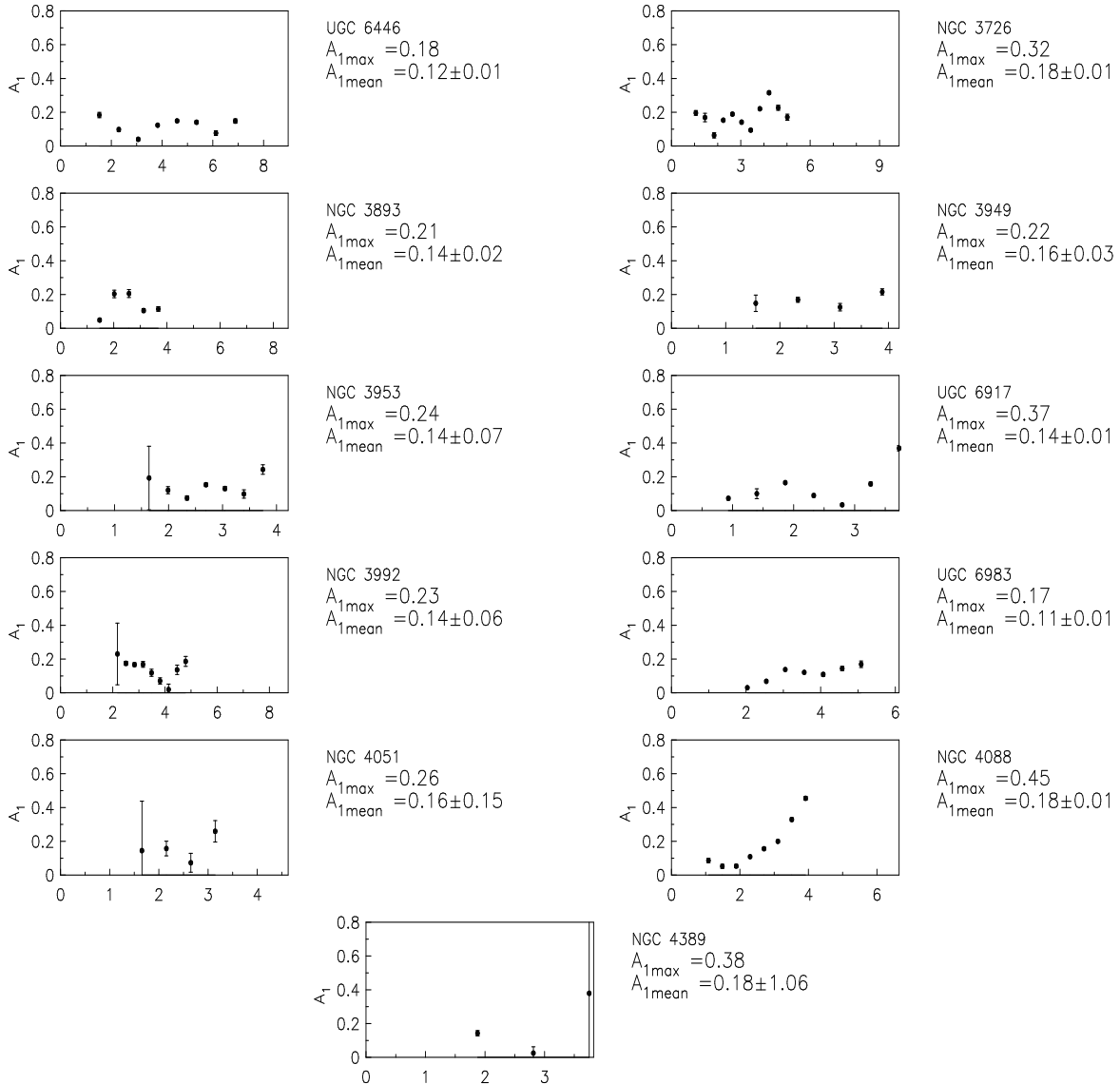


Figure 1. The asymmetry parameter derived from the surface density maps (moment 0). In each of the maps, the radius is in the units of K'-band scale length. The mean value estimated is for the complete range.

In contrast, the advanced mergers of galaxies show an amplitude A_1 that peaks at an intermediate radius of a few kpc and then turns over, and the phase shows a large fluctuation with radius (Jog & Maybhate 2006). These two different properties clearly underline the different mechanism for the origin of lopsidedness in the present sample of normal galaxies as compared to the mergers of galaxies.

(ii) The average value of the lopsidedness is $\sim 0.14 \pm 0.05$ (Table 2, column 4). This is similar to the mean value for the field galaxies obtained over the same radial region of 1.5-2.5 disk scalelengths (Rix & Zaritsky 1995, Bournaud et al. 2005) and about half of the average value that is seen in the Eridanus group (Paper I). In addition, only 2 out of the 11 galaxies (or $\sim 20\%$) of this sample have $A_1 \geq 0.2$ and none have $A_1 \geq 0.3$. On the other hand, the Eridanus group of galaxies (Paper I) showed higher values ($\sim 40\%$ and $\sim 30\%$ of the sample had A_1 values higher than 0.2 and 0.3 respectively).

Thus, despite being in a group environment, the Ursa Major galaxies show overall smaller A_1 values; this point is highlighted in Figure 3 where histograms for the A_1 values for the Ursa Major and Eridanus groups are plotted. To verify that this is not a spurious effect due to the limited size of the samples, we have carried out Kolmogorov-Smirnov (KS) test on the data samples, including 3 values of A_1 estimated from R-Band analysis (see Discussion). The D statistics value was estimated to be 0.357. The probability that the two samples come from the same distribution is 23.6%. This points to a different physical reason for the origin of the observed lopsidedness in this group (see Section 4 for a detailed discussion).

(iii) In addition, since the HI extends much farther out and can be studied to a larger radii than the stars, we have measured A_1 values to larger radial range going up to 4-6 disc scalelengths as compared to 2.5 disc scalelengths possi-

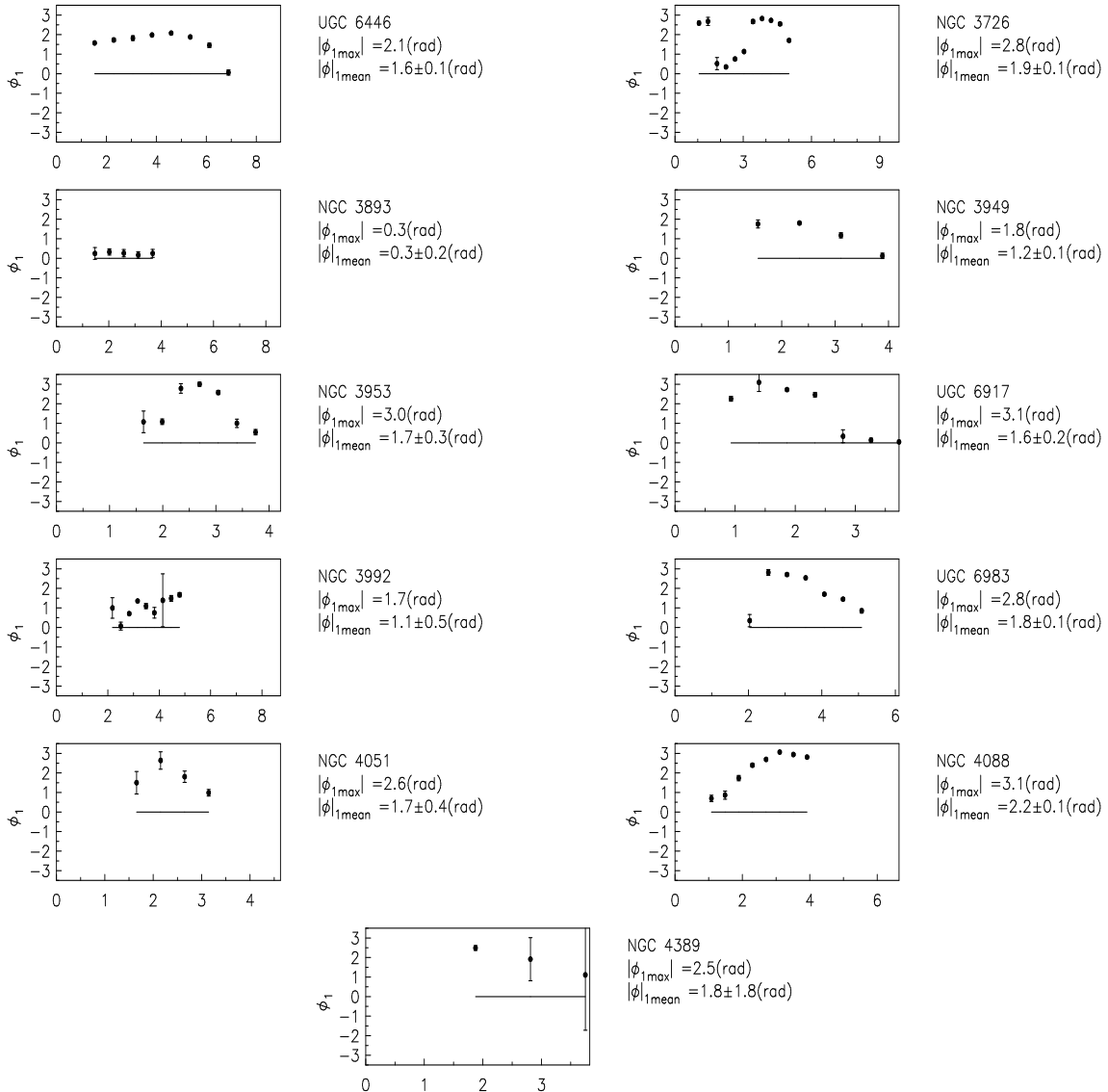


Figure 2. The asymmetry phase parameter derived from the surface density maps (moment 0). In each of the maps, the radius is in the units of K'-band scale length.

ble in the stellar case (Rix & Zaritsky 1995, also see Section 3.2 in the present paper).

(iv) The values of asymmetry as measured by the Fourier amplitudes A_1 , A_2 , and A_3 over the range $1-2 R_w$ (see Table 2) are comparable. In contrast, the field galaxies show the amplitudes A_1 and A_2 for $m=1,2$ to be stronger than A_3 for $m=3$ in general (Rix & Zaritsky 1995, Bournaud et al. 2005), and in centres of advanced mergers it was found that A_3 is large only when A_1 is large, and in any case the A_3 values are always smaller than the A_1 values (Jog & Maybhate 2006). The similar values of the amplitudes of $m=1,2,3$ in the Ursa Major case could be due to the complex group potential with possible multiple interactions which may be reflected in the amplitudes of $m=3$ and higher modes.

3.1.2 Kinematical Lopsidedness in HI

The five parameters i.e. the coordinates of the centre (x_0, y_0), systemic velocity (V_0), circular velocity (V_c), inclination (i) and the position angle (PA), estimated from the velocity maps using the iterative use of GIPSY routine ROTCUR. These parameters were given as the input to another GIPSY routine called RESWRI along with the velocity maps and the HI-surface density maps to obtain the harmonic coefficients.

At each radii (r), the line of sight velocity was expanded in the form

$$v_{los}(r, \phi') = c_0 + \sum_{m=1} c_m \cos(m\phi') + s_m \sin(m\phi') \quad (5)$$

where, c_m, s_m are the harmonic coefficients, c_0 is identical to the systemic velocity V_0 and ϕ' is the azimuthal angle. These harmonic coefficients were derived at concentric radii which were separated by $15''$. In our analysis we have derived

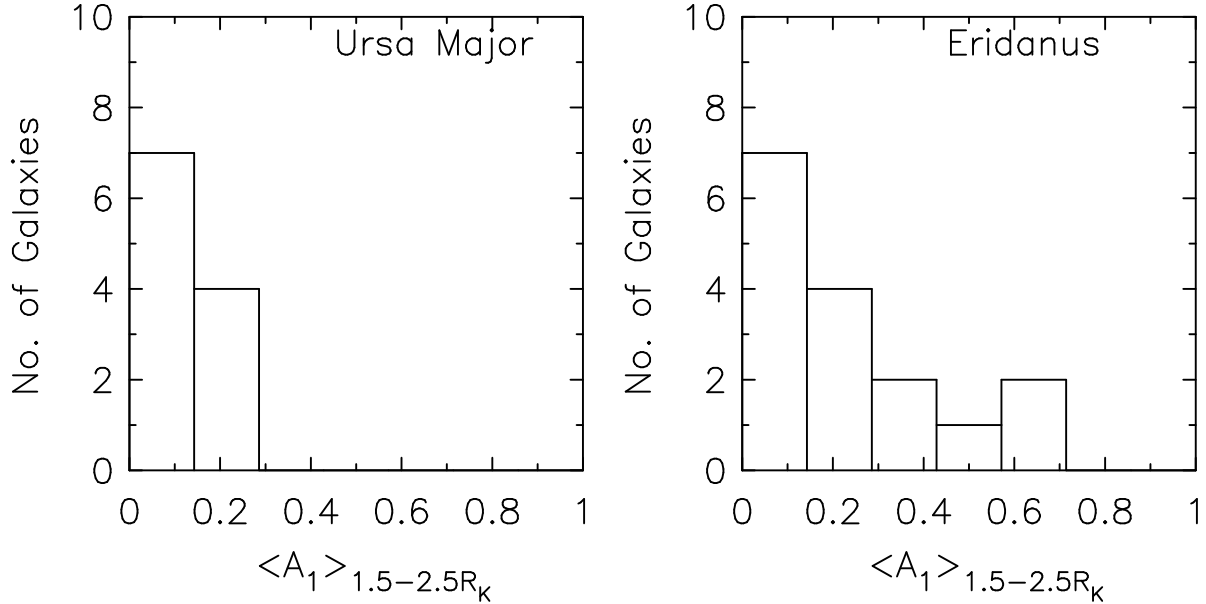


Figure 3. The histograms showing the number of galaxies vs. $\langle A_1 \rangle$ in the 1.5 to $2.5 R_K'$ range for the Ursa Major Group (left) and the Eridanus Group (right) of galaxies. Clearly, the Ursa Major galaxies show overall smaller amplitudes of lopsidedness.

Table 2. The mean values of A_1 in the range 1.5 to $2.5 R_K'$, and A_1, A_2, A_3 in the range 1 to $2 R_w$

Name	Hubble Type	$R_{K'}$ (kpc)	$\langle A_1 \rangle_{K'}$ $1.5 - 2.5 R_K'$	R_w (kpc)	$\langle A_1 \rangle_w$ $1 - 2 R_w$	$\langle A_2 \rangle_w$ $1 - 2 R_w$	$\langle A_3 \rangle_w$ $1 - 2 R_w$
UGC 6446	7	0.82	0.14	3.19	0.17	0.23	0.08
NGC 3726	5	2.12	0.11	4.08	0.16	0.12	0.12
NGC 3893	5	1.70	0.20	--	--	--	--
NGC 3949	4	1.00	0.16	2.69	0.22	0.27	0.07
NGC 3953	4	2.90	0.13	3.96	0.17	0.28	0.17
UGC 6917	7	1.90	0.13	3.80	0.13	0.21	0.06
NGC 3992	4	3.11	0.23	--	--	--	--
UGC 6983	6	2.06	0.03	4.43	0.13	0.07	0.11
NGC 4051	4	1.37	0.15	2.86	0.17	0.25	0.14
NGC 4088	4	1.81	0.08	4.13	0.19	0.18	0.11
NGC 4389	4	0.74	0.14	--	--	--	--
Mean			0.14 ± 0.05		0.17 ± 0.03	0.20 ± 0.07	0.11 ± 0.04

the harmonic coefficients up to the 10^{th} order. This was partially prompted by the observation that effects of bars tend to retain the strength of the Fourier coefficients even for $m=10$ terms (Buta et al. 2003). Typical velocity harmonic coefficients are shown in Figure 4.

From these coefficients, since $c_3 \sim 0$, it is seen that the inclination fitting has converged (Schoenmakers et al. 1997). In addition, an estimate of the effects of spiral arms and global elongation in the potential that gives rise to the kinematical lopsidedness can be obtained from the s_1 & s_3 coefficients (Schoenmakers et al. 1997). If the influence of spiral arms are large, s_1 and s_3 are expected to oscillate rapidly (Schoenmakers et al. 1997). Since this is not seen in Figure 4, their contribution must be small.

From the harmonic coefficients thus obtained, it is possible to estimate the elongation in the potential of the galaxy

times a factor of $\sin(2\phi_2)$, where ϕ_2 is the phase angle for $m = 2$ in the plane of the galaxy (Schoenmakers et al. 1997). The estimation of the ellipticity of the potential of an early type galaxy, IC 2006, using the velocity field for the HI ring in it was first carried out by Franx et al. (1994). This was later generalised to include spiral galaxies with extended exponential disks (Schoenmakers et al. 1997). In this procedure, with the assumptions of flat rotation curve in the outer regions of the galaxy and constant phase ($\phi_2(r)$), the ellipticity of potential (ϵ_{pot}) is obtained as $\epsilon_2 \sin(2\phi_2(r))$ (Schoenmakers et al. 1997). We have carried out similar analysis for all the sample galaxies in the Ursa Major group, and presented in Section 3.3. A typical asymmetry or the elongation in the potential for NGC 3726 is shown in Figure 5.

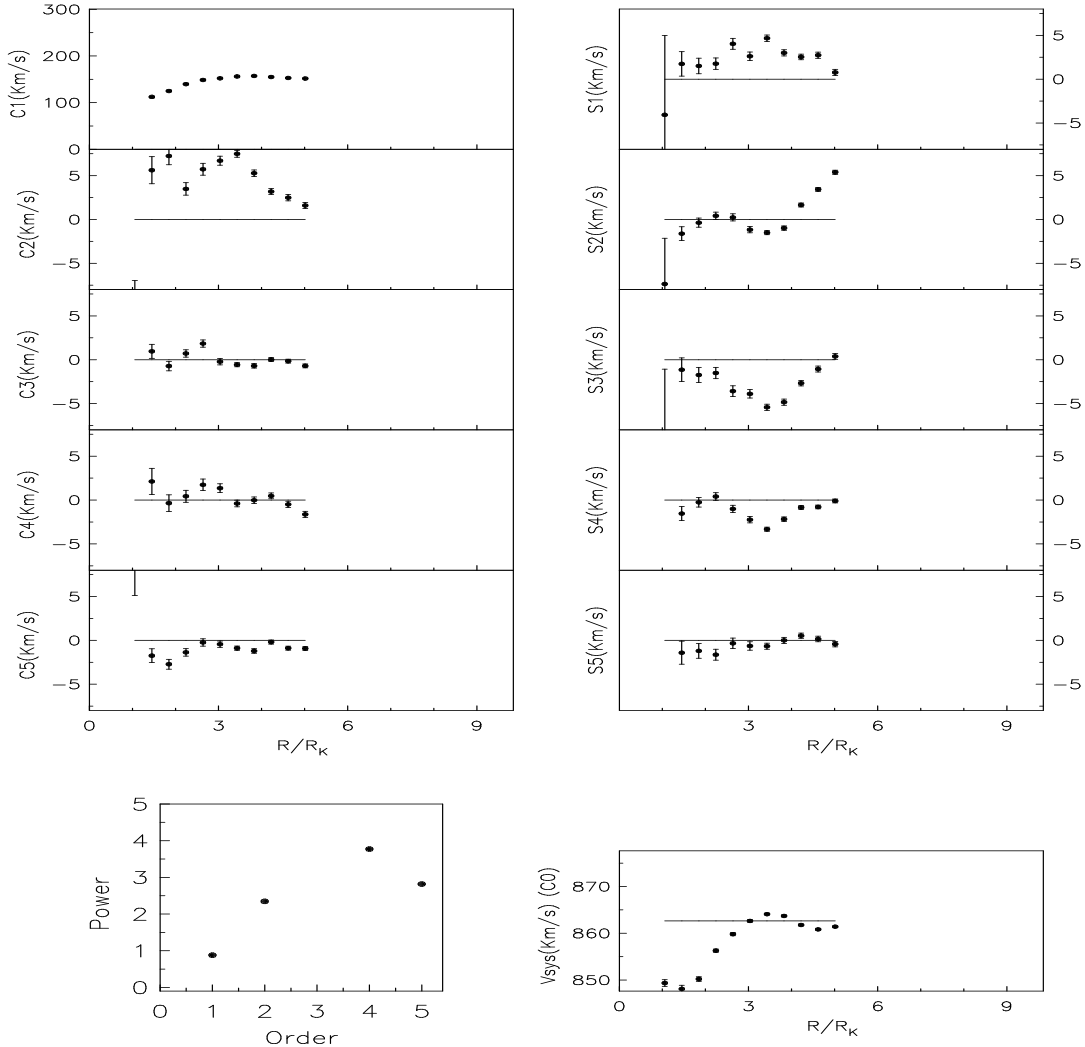


Figure 4. Velocity harmonic coefficients estimated for NGC 3726. The power in each of the harmonic order is shown in the bottom left hand panel. The bottom right hand panel shows the c_0 coefficient (V_{sys}) as a function of radius.

3.2 Harmonic Analysis of Optical and Near-IR Data

The harmonic analysis of the optical (R-band and K'-band) data was carried out as per the procedure adopted by earlier workers (Rix & Zaritsky 1995; Zaritsky & Rix, 1997; Paper I 2006). The original images obtained from CADC were corrected for the sky background and for the atmospheric extinction. In addition to this, foreground stars were masked. The optical centres of the galaxies were estimated using the IRAF task IMCNTR. It was seen that the optical centres of these galaxies were the same as that obtained by Tully et al. (1996). These images were deprojected using

the IRAF¹ task IMLINTRAN (Buta et al. 1998). In this deprojection, we have not taken into account the effects of the bulge of the galaxy. The effect of bulge is expected to be very small as we are mainly interested in the outer regions of the galaxy (Bournaud et al. 2005). In addition we expect bulge contamination to be serious for the $m=2$ mode and for almost edge-on galaxies which is not relevant in our case. For each of the galaxies, along various concentric annuli, the surface density as a function of angle was extracted

¹ IRAF is distributed by the National Optical Astronomy Observatories, which are operated by the Association of Universities for Research in Astronomy, Inc., under cooperative agreement with the National Science Foundation.

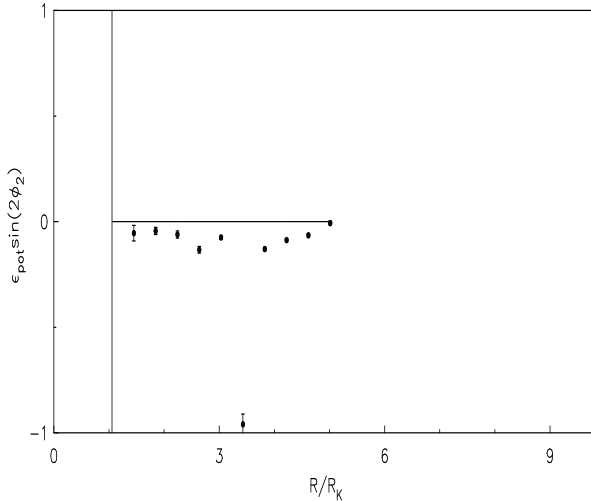


Figure 5. The estimated elongation in potential $\epsilon_{pot} = \epsilon_2 \sin(2\phi)$ derived from the velocity harmonic coefficients for NGC 3726

using the ELLIPSE² task. Each of the rings were separated by 1'' (typical resolution) in the case of R-Band images. Harmonic analysis was carried out on the extracted surface density values and normalised coefficients were estimated. The variation of A_1 coefficients, derived from R-Band image along with those derived from the HI analysis for two sample galaxies NGC 3726, NGC 4051 are shown in Figure 6.

From this figure, it can be seen that the lopsidedness in the stellar distribution measured from the optical data is comparable to that seen in HI in the same radial region of study. Thus these values represent true lopsidedness and not features seen only for the kind of tracer used. This agreement confirms what was also seen in our earlier study of HI lopsidedness in Eridanus (Paper I), and provides evidence that the asymmetry in both arise due to the stars and gas responding respectively to the same perturbation potential as proposed by Jog (1997). In the outer parts, only HI is available as a tracer since the near-IR data is available only up to 2.5 disc scalelengths (see Section 3.1.1).

3.3 Strength of the Perturbation Potential

Assuming that the asymmetry arises due to the disc response to a distorted halo (Jog 1997), from the surface density maps, we can obtain the perturbation potential corresponding to the $m=1,2,3$ terms from the observed amplitudes A_1 , A_2 and A_3 for the normalised Fourier coefficients (Jog 2000). Here the perturbation potential is taken to be of the form $V_c^2 \epsilon_m \cos m\phi$ where V_c is the flat rotation curve value and ϵ_m denotes the perturbation parameter. As a result, it can be shown that ϵ_1 denotes the lopsided potential, and ϵ_2 denotes the elongation or ellipticity of the perturbation potential.

The observed HI distribution was fitted with a Gaussian curve and the associated *Gaussian scalelength* R_w was estimated. Using this scalelength the relations between ϵ_m ,

A_m and R_w have been derived for $m = 1, 2$ and 3 , following the procedure in Jog (2000) where it was developed for an exponential disk distribution in a region of flat rotation curve. It is now believed that haloes of galaxies in groups are merged in the outer parts (Athanassoula et al. 1997), however in the inner regions of 10 kpc where we study the asymmetry, we can still treat the asymmetry as if the halo were isolated. Hence the above model of disk response to a halo is still reasonably valid and the inner regions could carry the signatures of complex tidal interactions in a group setting. This yields the following relations between the perturbation parameters for the potential ϵ_m and the A_m values:

$$\epsilon_2 = \frac{A_2(r)}{(r/R_w)^2 + 1} \quad (6)$$

and

$$\epsilon_3 = \frac{A_3(r)}{(2/7)(r/R_w)^2 + 1} \quad (7)$$

The relation for $m=1$ was already obtained in Paper I, and is:

$$\epsilon_1 = \frac{A_1(r)}{2(r/R_w)^2 - 1} \quad (8)$$

The resulting mean values of the perturbation parameters are obtained using the measured values of the Fourier amplitudes A_1 , A_2 and A_3 , and are given in Table 3.

Using the analysis of the kinematical data, we have also obtained $\epsilon_2 \sin[2\phi_2(r)]$ for the galaxies in Ursa Major as discussed in Section 3.1.1. The mean values of this quantity in the range 1-2 R_w are shown in Table 3.

The main results from this subsection are:

- (i) The average value of ϵ_1 or the lopsided perturbation for the potential obtained in the outer parts (in the radial range 1-2 R_w) is $\sim 6\%$, this is smaller than the value for the Eridanus case where the halo lopsided potential was derived to be 10% - this reflects the smaller observed amplitudes of lopsidedness in the present sample.

Thus if the lopsidedness is due to the response to the halo distortion, then this gives 6% as the typical halo lopsidedness for the Ursa Major galaxies.

² ELLIPSE is a product of the Space Telescope Science Institute, which is operated by AURA for NASA.

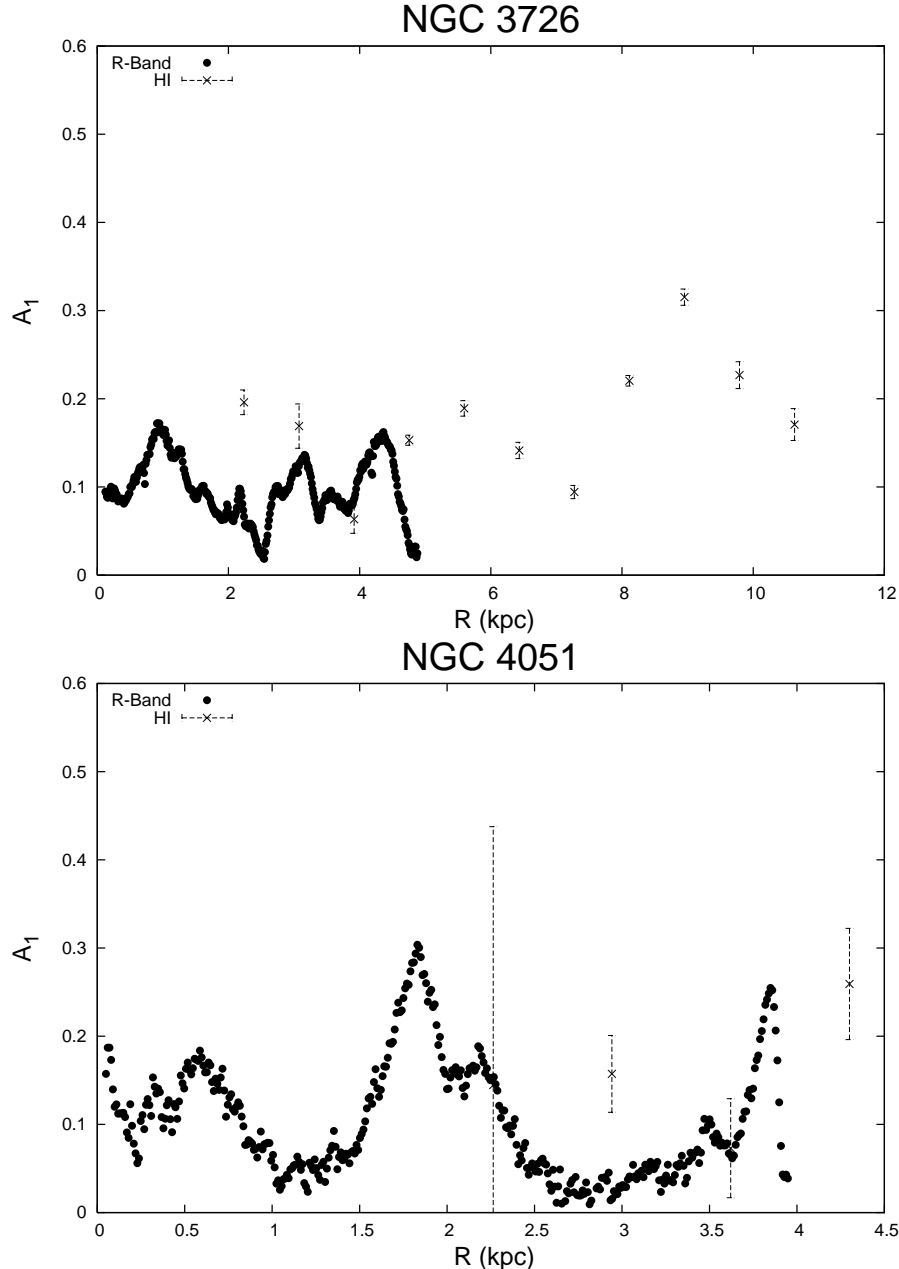


Figure 6. The A_1 coefficients derived from R-Band images of galaxies, which are compared with that obtained from HI surface density maps. Note that the values are comparable in the inner regions of radial overlap.

(ii) The elongation in the potential or the magnitude or the amplitude of the elongation in the term ϵ_2 value is comparable (within a factor of $\sin(2\phi_2)$) whether calculated from the observed spatial asymmetry or from the kinematical asymmetry (see columns 4 and 6 of Table 3). This confirms the argument (Jog 1997, Jog 2002) that both spatial and kinematical asymmetry result from the same perturbation potential.

(iii) The values of all three perturbation potentials derived $\epsilon_1, \epsilon_2, \epsilon_3$ are comparable. Although this result depends on the model used, it reinforces the similar result obtained for the Fourier amplitudes which are directly observed and hence are model-independent (Section 3.1.1). This can be an important clue to the mechanism for generating lopsidedness

in groups, and perhaps indicates the importance of multiple simultaneous tidal interactions that can occur under the special conditions of a group environment.

4 DISCUSSION : LOPSIDEDNESS IN GROUPS

(i) The Ursa Major group of galaxies show a typical lopsidedness of $\sim 14\%$ in the inner regions, that is comparable to the field case, and about half of what is seen in the Eridanus group (see Section 3.1.1 for details).

We also measure the A_1 values in the outer parts between 1-2 R_w , and find this to be $\sim 17\%$. Again this is smaller by a factor of ~ 1.6 compared to the Eridanus case.

Table 3. The HI-scalelength, and the mean perturbation parameters of potentials obtained from A_1 , A_2 and A_3 - the coefficients of surface densities and from velocity fields. The mean values are calculated between 1-2 R_w

Name	HI Scalelength (R_w) (kpc)	$\langle \epsilon_1 \rangle$	$\langle \epsilon_2 \rangle$	$\langle \epsilon_3 \rangle$	$\langle \epsilon_2 \sin(2\phi_2) \rangle$
UGC 6446	3.19	0.046	0.040	0.065	-0.173
NGC 3726	4.08	0.049	0.042	0.111	-0.392
NGC 3949	2.69	0.072	0.106	0.056	0.178
NGC 3953	3.96	0.044	0.098	0.113	-0.171
UGC 6917	3.80	0.041	0.057	0.083	0.007
UGC 6983	4.43	0.032	0.022	0.128	-0.213
NGC 4051	2.86	0.082	0.113	0.109	-0.087
NGC 4088	4.13	0.089	0.076	0.092	0.001
Mean		0.057 ± 0.021	0.069 ± 0.034	0.095 ± 0.025	-0.106 ± 0.172

(ii) We plot the mean A_1 ($\langle A_1 \rangle$) value in the inner regions of the galaxies with respect to Hubble type in Figure 7, where we also plot the corresponding values from the Eridanus study for comparison (Paper I, Figure 5). Note that the early-type galaxies in the Eridanus group show a higher lopsidedness, this is opposite to what is seen in the field galaxies (Zaritsky & Rix, 1997; Bournaud et al. 2005), and points to tidal interactions as the mechanism for the origin of lopsidedness as argued in Paper I. In contrast, in field galaxies, gas accretion plays an important role in generating lopsidedness (Bournaud et al. 2005). The anti-correlation with galaxy Hubble type is weaker in the Ursa group case, perhaps because our sample here only covers a smaller subgroup of galaxy types from type 4 to 7, whereas the Eridanus study spans a much larger range from type 1 to 9.

To address this issue, we obtained the R-Band images of three more galaxies from the Ursa Major sample (Tully et al. 1996), namely UGC 6930, NGC 4102 and NGC 3729, from the Canadian Astronomy Data Centre (CADC) on which Fourier analysis was carried out. UGC 6930 belonged to Hubble type 7 and had an inclination of 32° . NGC 4102 and NGC 3729 belonged to Hubble type 2 and had inclinations 58° and 48° respectively. The A_1 coefficient in the range 1.5 to $2.5 R_{K'}$ for UGC 6930 was estimated to be 0.02. In the same range, the A_1 coefficients for NGC 4102 and NGC 3729 were 0.12 and 0.04 respectively. These galaxies were not included in our HI analysis because of lack of reliable HI data. It should be noted that if these three points are included in KS-test, the probability that the values of A_1 come from the same distribution is 23.6% while the maximum difference (D) between the cumulative distribution is 0.357. The three resulting points are shown in Fig. 7 (denoted by symbol Δ) and they confirm that the distribution of A_1 vs. R is nearly flat. Thus there is no clear anti-correlation in this case unlike that seen in the Eridanus group. However, this distribution does not show a positive correlation with the Hubble type either, unlike the field case (Bournaud et al. 2005). Thus Figure 7 confirms the different physical origins for the lopsidedness in the group and field cases. It also confirms that the anti-correlation seen in the Eridanus group can be attributed to the group environment, and requires a higher galaxy number density as seen in the Eridanus to be effective.

(iii) The kinematical analysis gives a value for the elongation in the potential, showing all galaxies where such analysis could be carried out to be disturbed. This was found earlier for a group of five galaxies in the Sculptor group galaxies (Schoenmakers 2000).

(iv) The above results show that the group environment is conducive to producing lopsidedness, with tidal interactions playing a major role in this. Galaxy interactions can give rise both to lopsidedness and a secular evolution towards early-type galaxies as argued by Bournaud et al. (2005). There are indeed some indications of tidal interactions in Ursa Major group of galaxies (Verheijen & Sancisi 2001).

The Ursa Major group is a loose group, and has number density that is intermediate between the field and the Eridanus values. Hence tidal interactions are less important in the Ursa Major group, which could explain the lower amplitude of lopsidedness (A_1).

The lower values of asymmetry parameter ($\langle A_1 \rangle$) observed for Ursa Major group of galaxies may also find a partial explanation, if we assume that it mainly falls on a filament and is in the process of forming a group. Such a process is observed in ZwCl 2341.1+0000 (Bagchi et al. 2002).

5 CONCLUSIONS

The main conclusions drawn from this paper are as follows:

(i) The mean amplitude of disk lopsidedness in the Ursa Major group galaxies is measured and found to be comparable to the field sample, while the Eridanus group showed a factor of two higher lopsidedness.

The smaller amplitudes of lopsidedness seen in the present study could be due to the lower galaxy number density and the lower velocity dispersion in the Ursa Major group (see Section 2). The group environment and tidal interactions are shown to play a major role in generating lopsidedness, especially in a denser group like the Eridanus.

The disk lopsidedness can thus be used as diagnostics to study the galaxy interactions and the halo properties in groups of galaxies.

(ii) The values of elongation of potential as measured from spatial and kinematical studies gives comparable val-

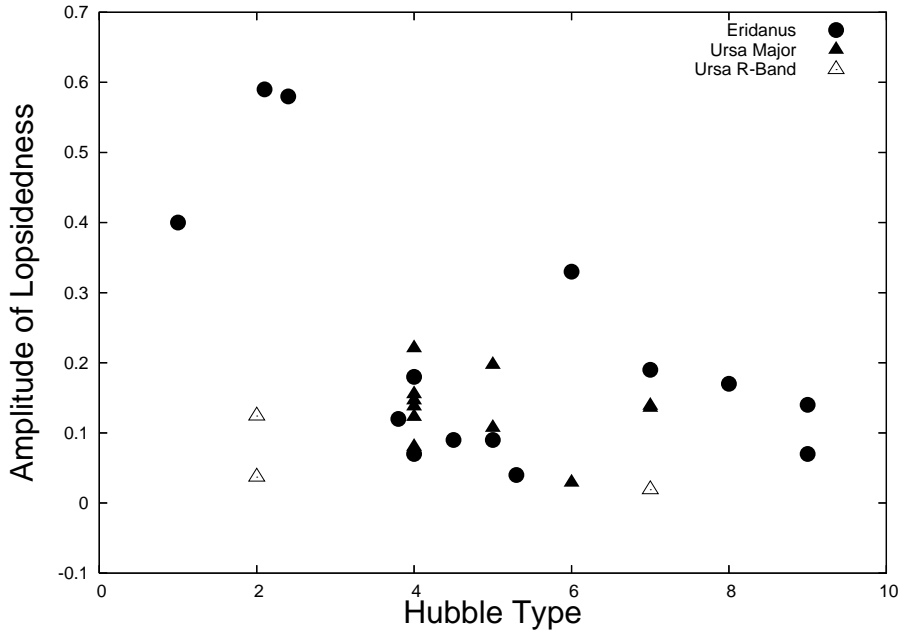


Figure 7. The $\langle A_1 \rangle$ values in the 1.5 to 2.5 K'-band scale length of Ursa Major galaxies. The Eridanus Group values are taken from Paper I. The values denoted by Δ , correspond to A_1 values of the 3 galaxies estimated from R-Band analysis (see Discussion). The A_1 values are higher for the early-type galaxies in the Eridanus while the distribution is flatter for the Ursa Major group.

ues, thus supporting the idea (Jog 1997) that both types of asymmetry arise due to the same perturbation potential.

(iii) The values of the asymmetry as measured by the mean fractional Fourier amplitudes A_1 , A_2 and A_3 are found to be comparable, and also the derived perturbation potential parameters ϵ_1 , ϵ_2 and ϵ_3 are found to be comparable. This is in contrast to the field galaxies where A_1 and A_2 are stronger than A_3 and higher mode amplitudes. This indicates the importance of multiple tidal interactions that can occur under the special conditions of a group environment.

6 ACKNOWLEDGMENTS

We thank the referee, Frederic Bournaud, for a careful reading of the manuscript and for the critical comments and the suggestion of including the A_1 values from R-Band images in Figure 7. These have improved the presentation of the paper. RAA takes great pleasure in thanking K. Indulekha, School of Pure and Applied Physics, M.G.University,for her constant encouragement during this project. He also thanks the University Grants Commission of India and St.Joseph's College, Bangalore for granting study leave under the FIP leave of 10th five year plan and Raman Research Institute, Bangalore for providing all the facilities to pursue this study. This research used the facilities of the Canadian Astronomy Data Centre operated by the National Research Council of Canada with the support of the Canadian Space Agency.

REFERENCES

Angiras,R.A., Jog,C.J., Omar,A., Dwarakanath,K.S., 2006, MNRAS, 369, 1849 (Paper I)

Athanssoula,E., Makino,J., Bosma,A., 1997, MNRAS, 286, 825

Baldwin,J.E., Lynden-Bell,D., Sancisi,R., 1980, MNRAS, 193, 313

Bagchi,J., Enlin,.A, Miniati,.O, Stalin,C. S., Singh,M., Raychaudhury,.S, Humeshkar,N.B., 2002, NewA., 7, 249

Block, D. L., Bournaud, F., Combes, F., Puerari, I., Buta, R. A&A, 2002, 394, L35

Bournaud,F., Combes,F., Jog,C.J., Puerari,I., 2005, A&A, 438, 507

Buta R., Alpert A.J., Cobb M.L., Crocker D.A., Purcell G.B., 1998, AJ, 116, 1142

Buta R., Block D.L., Knapen J.H., 2003, AJ, 126, 1148

Franx M., van Gorkom J.M., de Zeeuw P.T., 1994, ApJ, 436, 642

Haynes, M.P., Hogg, D.E., Maddalena, R.J., Roberts M.S., van Zee, L. 1998, AJ, 115, 62

Jog,C.J., 1997, ApJ, 488, 642

Jog,C.J., 2000, ApJ, 542, 216

Jog,C.J., 2002, A&A, 391, 471

Jog, C.J., Maybhate, A. 2006, MNRAS, 370, 891

Matthews,L.D., van Driel W., Gallagher,J.S., 1998, AJ, 116, 1169

Noordermeer,E., Sparke,L.S., Levine,S.E., 2001, MNRAS, 328, 1064

Omar,A., Dwarakanath,K.S., 2005a, JA&A, 26, 1

Omar,A., Dwarakanath,K.S., 2005a, JA&A, 26, 71

Rasmussen J., Ponman T.J., Mulchaey J.S., Miles T.A., Raychaudhury S., 2006, MNRAS, 373, 653

Richter,O.-G., Sancisi,R., 1994, A&A, 290, L9

Rix,H.-W., Zaritsky,D., 1995, ApJ, 447, 82

Schoenmakers R.H.M., Franx M., de Zeeuw P.T., 1997, MNRAS, 292, 349

Schoenmakers, R.H.M., 1999, in Valtonen, M., Flynn, C., eds., ASP Conf. Series, Vol. 209, Small Galaxy Groups,

Astron. Soc. Pac., San Francisco, pg. 54
Tully,R.B., Verheijen,M.A.W., Pierce,M.J., Huang,J.S.,
Wainscoat,R.J., 1996, AJ, 112, 2471
Verheijen,M.A.W., Sancisi,R., 2001, A&A, 370, 765
Wong,T., Blitz, L., Bosma,A., 2003, ApJ, 605, 183
Zaritsky,D., Rix,H.-W., 1997, ApJ, 447, 118